Hindawi
Advances in Materials Science and Engineering
Volume 2019, Article ID 9754528, 6 pages
https://doi.org/10.1155/2019/9754528

Research Article

Pickling Behavior of Duplex Stainless Steel 2205 in Hydrochloric Acid Solution

Huaying Li[1,2] **and Aichun Zhao**[1,2]

[1]*School of Materials Science and Engineering, Taiyuan University of Science and Technology, Taiyuan 030024, China*
[2]*Collaborative Innovation Centre of Taiyuan Heavy Machinery Equipment, Taiyuan University of Science and Technology, Taiyuan 030024, China*

Correspondence should be addressed to Huaying Li; lihy@tyust.edu.cn and Aichun Zhao; zhaoaichun1985@126.com

Received 9 October 2018; Accepted 31 December 2018; Published 25 February 2019

Academic Editor: Yuanshi Li

The oxide-scale structure and pickling behavior of oxided 2205 duplex stainless steel in the electrolytes containing hydrochloric acid were investigated. The oxide scales mainly consist of two layers: the outer layer is dense Fe_2O_3, and the inner granular is $FeCr_2O_4$ spinel. During the pickling process, pittings form around the boundaries of $FeCr_2O_4$ particles or interfaces of two kinds of oxides, which results in that the electrolyte can directly react with the chromium-depleted layer along the pittings to produce an "undercut" effect so that the pickling efficiency is improved markedly. The pickling mechanism was discussed, and the model was established.

1. Introduction

Duplex stainless steel 2205 is one of the most common kinds of DSSs with the volume fraction of each phase above 30%. Due to the proper austenite-ferrite balance, 2205 exhibits exceptional corrosion resistance properties except for excellent strength and impact toughness [1, 2] and thus has been widely used in oil and gas exploration, shipping preparation, flue gas desulfurization, desalination, and other industrial fields [3–6].

Pickling is one of the most important steps in the manufacture of 2205 and can become the limiting factor of production efficiency. Pickling of 2205 is very difficult for four reasons. Firstly, the oxide scales on 2205 are dense and adherent strongly to the underlying metal. Secondly, the removal of the chromium-depleted layer beneath the oxide scales is imperative due to its low corrosion resistance [7–10]. Thirdly, the alloying element contained in 2205, such as molybdenum and nitrogen, can improve the stability of the oxide scales remarkably [11]. Fourthly, the composition, thickness, and protectiveness of the oxide scales formed on the austenitic phase and ferritic phase are not the same due to the different chromium contents in them [12–14].

Researches [15] have shown that electrolytes containing hydrochloric acid can efficiently remove the chromium-depleted layer for hot-rolled 304 due to the anodic brightening mechanism [16]. But whether the hydrochloric acid can improve the pickling efficiency of 2205 is still not clear. Moreover, the researches on the pickling of 2205 mainly focus on the electrochemical pickling [17–19], and little work has been done on the chemical pickling. This paper mainly discussed the pickling behavior of 2205 in electrolytes containing hydrochloric acid and the evolution of the oxide scale by chemical pickling. Finally, a hydrochloric acid pickling model was built on these results.

2. Experiment Procedure

2205 duplex phase stainless steel (with a chemical composition of 0.018 wt.% C, 1.2 wt.% Mn, 22.6 wt.% Cr, 5.3 wt.% Ni, and balanced Fe) was hot rolled into a plate, following annealing and blasting treatment (called as oxidized 2205). Specimens (30 mm × 30 mm) were machined from the plater. The phase components of the oxide scale were investigated by a Japan Rigaku D/Max-IIIB X-ray diffractometer with Cu Kα1 radiation ($\lambda = 1.5405$ Å). The accelerating voltage,

emission current, and scanning speed were 40 kV, 40 mA, and 0.2°/s, respectively. The morphologies and microstructures of the specimens were observed using a UK Leica Cambridge S360 scanning electron microscope (SEM).

Analytical grade chemicals and distilled water were used to prepare the electrolyte containing 110 g/L HCl. And a little oxidant was added to the electrolyte to advertise overcorrosion. The tests were carried out at 80°C under the unstirred condition.

Corrosion potential during the pickling process was measured by an electrochemical workstation (PARSTAT® 2273, USA), and a saturated calomel electrode was used as the reference electrode. When the electrodes were introduced into the test electrolyte, the corrosion potential measurement started. Furthermore, some specimens were immersed into the same electrolyte and taken out after the following time intervals: 30 s, 60 s, and 90 s. Afterwards, the specimens were rinsed with distilled water to remove the residual electrolyte and dried to analyze the evolution process of the oxide scale in the pickling electrolyte by SEM. The specimen rinsed for 90 s was then slightly brushed to remove the residual oxides to observe the micromorphology of the matrix.

3. Results

3.1. Composition of Surface Oxide Scale. Figure 1 presents the X-ray diffraction pattern of the 2205 surface oxide scale. It clearly shows the typical diffraction peaks of the matrix indicating that the X-rays completely penetrated the oxide layer so that the possibility of undetected oxide phases was minimized. Moreover, the pattern reveals that the oxide scale consists of Fe_2O_3, $FeCr_2O_4$ spinel, and SiO_2, which is in accordance with the research of Li et al. [12].

3.2. Cross-sectional Morphology and Elements Distribution of Surface Oxide Scale. Figure 2 shows the SEM image of the cross-sectional morphology and the EDS maps showing the distribution of the main elements, which combine with oxygen to form the surface oxide scale. The thickness of the oxide scale is approximately 10 μm. And the scale can be divided into two layers: the outer layer of iron-rich oxidation and the inner layer of chromium-rich oxidation. And also some silicon oxides are mainly enriched at the interface of the chromium oxide and matrix. Combining this result with the X-ray spectra, it can be inferred that the outer layer is Fe_2O_3 and the inner layer is $FeCr_2O_4$ (a kind of spinel).

3.3. Corrosion Potential of Pickling Process. The corrosion potential of 2205 pickling in the electrolyte containing hydrochloric acid shows a typical characteristic of hydrochloric acid pickling [16] (Figure 3). In the initial stage, the corrosion potential decreases sharply as the electrolyte permeates the interface of the oxide scale and the chromium-depleted layer. The corrosion potential stays first at a low level after decreasing down and then abruptly increases up to a relatively high value after duration because of the dissolution of the chromium-depleted layer. This reflects an active-to-passive transition rather than an anodic brightening [16].

In addition, as shown in Figure 3, the whole pickling process lasted 60 s. However, the pickling process was kept for 90 s to ensure the uniformity of pickling in the immersion test.

3.4. Evolution Process of Oxide Scales in Pickling Electrolyte. The SEM images of the oxide scales after immersion in the pickling electrolyte for different times and the matrix after pickling are shown in Figure 4. The EDS results show that the outer layer of Fe_2O_3 is dense and the $FeCr_2O_4$ spinel stacking beneath the outer layer is granular. In the whole pickling process, the lumpy Fe_2O_3 had little changes, but the amount of $FeCr_2O_4$ decreased gradually. There were some cavities at the boundaries of the $FeCr_2O_4$ particles or the interfaces of two kinds of oxides (as indicated by the arrows). As the immersion time increased, the number and size of the cavities increased constantly. Up to 90 s, the surface oxide scale detached completely from the matrix, and the residual oxide could be easily removed by a nylon brush. The surface of the matrix after pickling was smooth without local pitting corrosion or other obvious corrosions, which can satisfy the requirements of cold rolling.

4. Discussion

Based on the XRD and EDS analysis results, it is known that the oxide scale is mainly composed of Fe_2O_3 and $FeCr_2O_4$. The reaction in the electrolyte containing hydrochloric acid is as follows:

$$Fe_2O_3 + 6H^+ = 2Fe^{3+} + 3H_2O \quad (1)$$

$$FeCr_2O_4 + 8H^+ = 2Cr^{3+} + Fe^{2+} + 4H_2O \quad (2)$$

The variations of the standard Gibbs free energy ΔG^θ for chemical reactions (1) and (2) at 80°C are 19.128 kJ and −63.122 kJ [20], respectively, suggesting that $FeCr_2O_4$ could be dissolved prior to Fe_2O_3 when immersed in the same reducing acid liquor. This accounts for why Fe_2O_3 shows little variation with the increase of time during the whole pickling process, while the $FeCr_2O_4$ spinel particles reduce with the increase of time.

The electrolyte contains a large amount of Cl^-, which can be preferentially adsorbed at the regions with higher energy, such as the boundary of the $FeCr_2O_4$ spinel and the interface of the two oxides. The adsorption of Cl^- promotes the dissolution of the oxides and the formation of cavities. The volume and depth of the cavities increase constantly with the increase of time till reaching the chromium-depleted layer. Then, the elements in the chromium-depleted layer react with the electrolyte as follows (taking Fe and Cr for example):

$$Fe + 2H^+ = Fe^{2+} + H_2\uparrow \quad (3)$$

$$Cr + 3H^+ = Cr^{3+} + 1.5H_2\uparrow \quad (4)$$

The variations of the standard Gibbs free energy ΔG^θ at 80°C are −91.283 kJ and −197.861 kJ, [20] respectively,

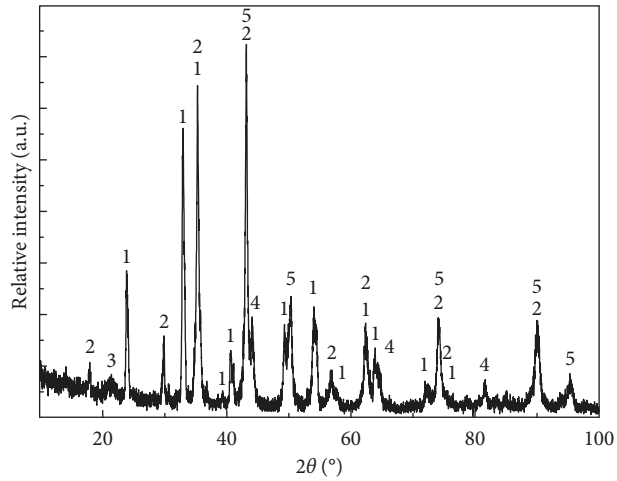

Figure 1: XRD pattern of the 2205 matrix and the surface oxide scale.

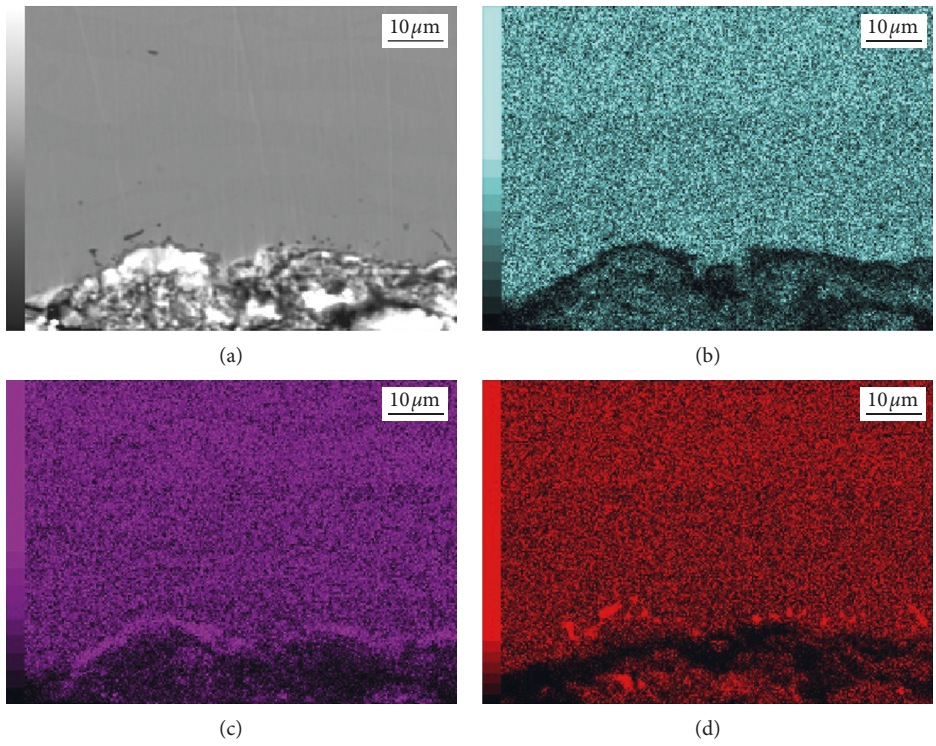

Figure 2: SEM images of the cross-sectional morphology (a) and EDS maps of Fe (b), Cr (c), and Si (d) for oxidized 2205.

meaning that the chromium-depleted layer will dissolve prior to the oxides. These reactions will produce an "undercut" effect on the oxide scale, and the reaction product H_2 can also degrade the integrality and adhesiveness of the oxide scale. Therefore, the oxide can be removed easily at the end of pickling.

According to the results above, a pickling mechanism model is built for the oxidized 2205 in hydrochloric acid solution, as shown in Figure 5. After hot rolling and high temperature annealing, the black-oxide scales on the surface of 2205 are integrated and compact (Figure 5(a)). The oxide scales consist of two layers: the outer layer is dense Fe_2O_3, and the inner is $FeCr_2O_4$. A thin chromium-depleted layer is formed between the inner oxide layer and matrix because of the formation of the oxide scales. After blasting, the outer Fe_2O_3 is mechanically ruptured and partially falls off from

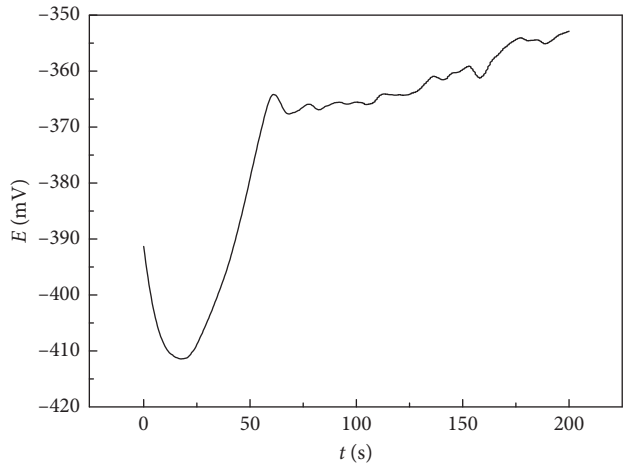

Figure 3: Corrosion potential of the oxidized 2205 in the electrolytes as a function of the pickling time at 80°C (containing 110 g/L HCl).

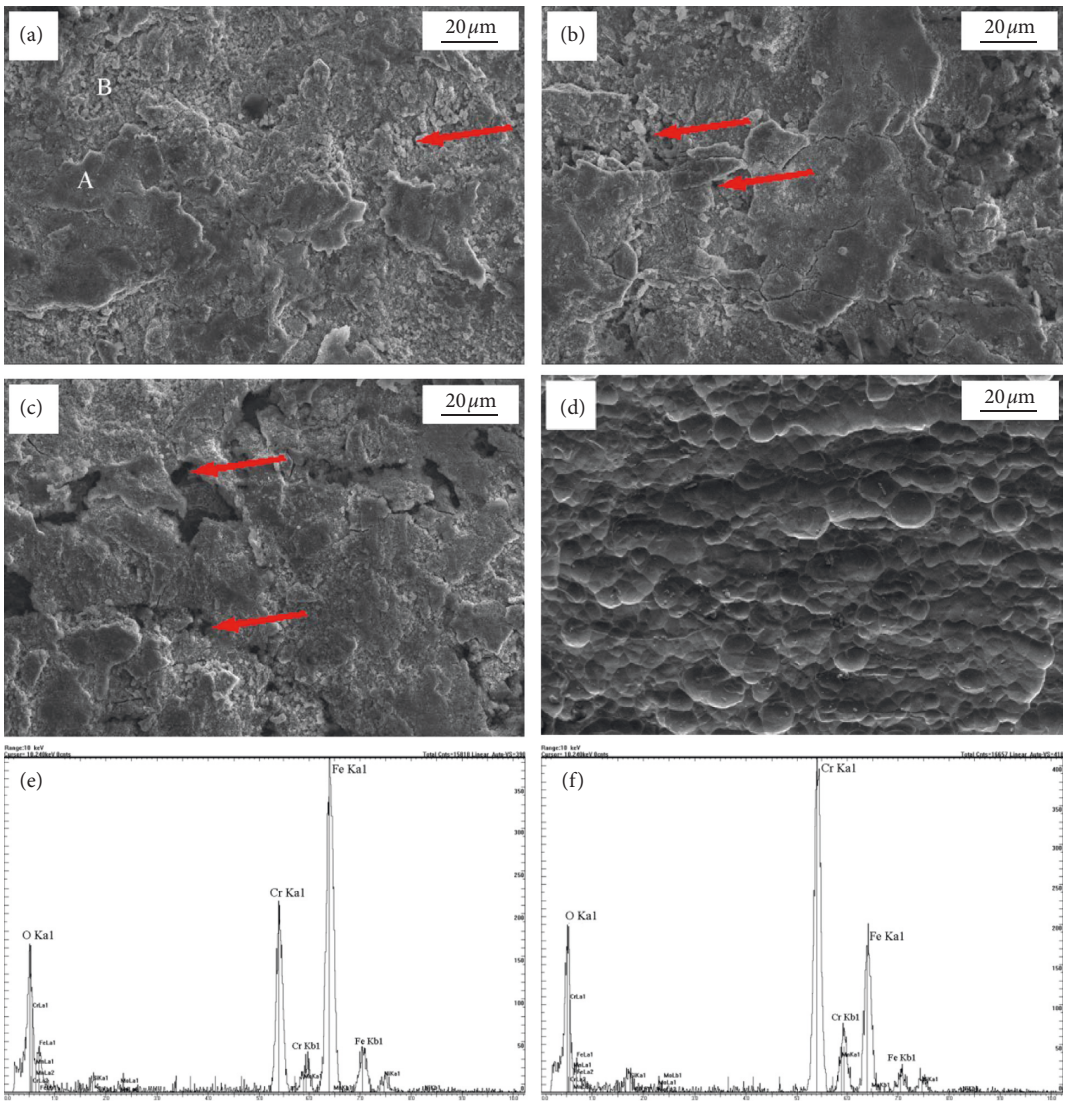

Figure 4: SEM images of the oxide scales after immersion in the pickling electrolyte for 30 s (a), 60 s (b), and 90 s (c), respectively. The matrix after pickling (d) and EDS spectrums corresponding to points A (e) and B (f) in (a), respectively.

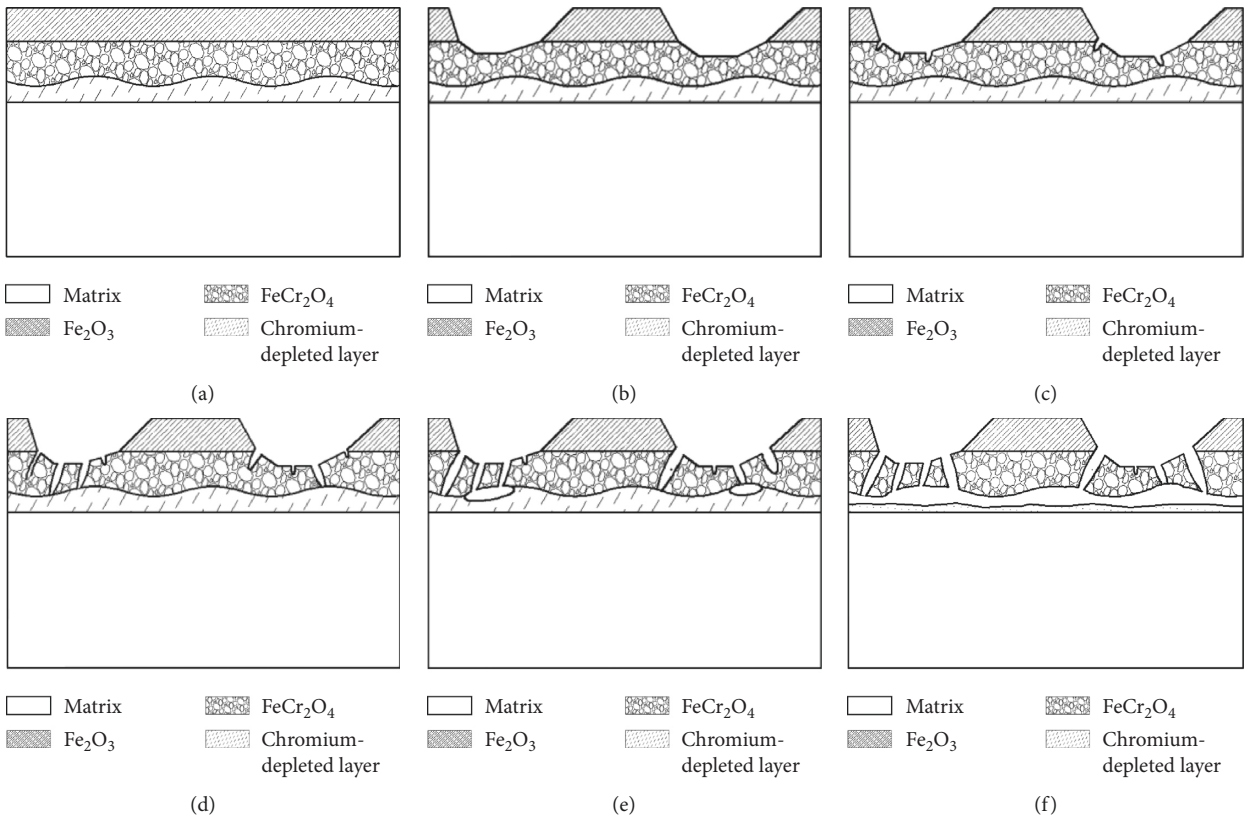

Figure 5: Schematics of the pickling process for oxidized 2205: (a) annealing; (b) shot blasting; (c) incubation period; (d) pitting period; (e) accelerated period; (f) end of pickling.

the surface and then the $FeCr_2O_4$ is exposed (Figure 5(b)). When immersed in the electrolyte, the oxidized stainless steel fully contacts with the solution. At the initial stage of pickling, Cl^- ions in the electrolyte are adsorbed at the boundaries of the $FeCr_2O_4$ particles and the interface of Fe_2O_3 and $FeCr_2O_4$, where pits nucleate (Figure 5(c)). According to the thermodynamic calculation, the electrolyte will preferentially react with $FeCr_2O_4$. Therefore, the $FeCr_2O_4$ crystals around the pit nucleus continuously dissolve, and the pits propagate along the grain boundaries to the matrix (Figure 5(d)). The electrolyte replenishes into the pits to maintain the continuous dissolution of the $FeCr_2O_4$ crystals. When the pits penetrate the oxide layer, the chromium-depleted layer is exposed to the electrolyte and preferentially reacts to dissolve. At this time, dissolution of the chromium-depleted layer becomes the main reaction of pickling and causes the "undercut" effect (Figure 5(e)). In addition, the hydrogen bubbles (not marked) generated can promote the fluidity of the electrolyte and mechanically damage the oxide scales. With prolongation of the pickling, the chromium-depleted layer is continuously dissolved until the whole oxide scale breaks away from the matrix, which indicates the end of the pickling process.

5. Conclusions

In conclusion, the oxide scales formed on the 2205 hot-rolled plate after annealing is mainly divided into two layers: the outer layer is the dense Fe_2O_3 crystal, and the inner is the granular $FeCr_2O_4$ spinel. The outer layer is broken after shot blasting treatment. When put in the electrolyte, the potential of the oxided 2205 decreases rapidly to the minimum value for some time and then gradually increases, showing obvious characteristics of hydrochloric acid pickling. During the pickling process, pittings are firstly formed around the boundaries of the $FeCr_2O_4$ particles or interfaces of the two kinds of oxides and then the electrolyte penetrates the oxide scales along the pittings to react with the chromium-depleted layer directly. This reaction produces an "undercut" effect so that the oxide scales are effectively removed.

Data Availability

The data used to support the findings of this study are available from the corresponding author upon request.

Conflicts of Interest

The authors declare that they have no conflicts of interest.

Acknowledgments

The present study was financially supported by the National Natural Science Foundation of China (51404159 and U1710257), International Science and Technology Cooperative Project of Shanxi Province, China (2015081011),

and Doctoral Research Foundation of Taiyuan University of Science and Technology, China (20142034 and 20142001). Also the Provincial Special Fund for Coordinative Innovation Center of Taiyuan Heavy Machinery Equipment is acknowledged.

References

[1] R. Huang, J. Wang, S. Zhong, M. Li, J. Xiong, and H. Fan, "Surface modification of 2205 duplex stainless steel by low temperature salt bath nitrocarburizing at 430°C," *Applied Surface Science*, vol. 271, pp. 93–97, 2013.

[2] Č. Donik, A. Kocijan, J. T. Grant, M. Jenko, A. Drenik, and B. Pihlar, "XPS study of duplex stainless steel oxidized by oxygen atoms," *Corrosion Science*, vol. 51, no. 4, pp. 827–832, 2009.

[3] A. Ruiz, N. Ortiz, A. Medina, J.-Y. Kim, and L. J. Jacobs, "Application of ultrasonic methods for early detection of thermal damage in 2205 duplex stainless steel," *NDT & E International*, vol. 54, pp. 19–26, 2013.

[4] A. Kashiwar, N. P. Vennela, S. L. Kamath, and R. K. Khatirkar, "Effect of solution annealing temperature on precipitation in 2205 duplex stainless steel," *Materials Characterization*, vol. 74, pp. 55–63, 2012.

[5] F. Zheng, T. Y. Cheng, and Q. Y. Zhang, "Production process for hot rolled strip of duplex stainless steel 2205," *Shanghai Nonferrous Metals*, vol. 30, pp. 31–33, 2009.

[6] H. Luo, C. F. Dong, K. Xiao, and X. G. Li, "Characterization of passive film on 2205 duplex stainless steel in sodium thiosulphate solution," *Applied Surface Science*, vol. 258, no. 1, pp. 631–639, 2011.

[7] L.-F. Li, P. Caenen, M. Daerden et al., "Mechanism of single and multiple step pickling of 304 stainless steel in acid electrolytes," *Corrosion Science*, vol. 47, no. 5, pp. 1307–1324, 2005.

[8] B. Ozturk and R. Matway, "Oxidation of type 304 stainless steels under simulated annealing conditions," *ISIJ International*, vol. 37, no. 2, pp. 169–175, 1997.

[9] L.-F. Li and J.-P. Celis, "Pickling of austenitic stainless steels (a review)," *Canadian Metallurgical Quarterly*, vol. 42, no. 3, pp. 365–376, 2013.

[10] J. Hildén, J. Virtanen, O. Forsén, and J. Aromaa, "Electrolytic pickling of stainless steel studied by electrochemical polarisation and DC resistance measurements combined with surface analysis," *Electrochimica Acta*, vol. 46, no. 24-25, pp. 3859–3866, 2001.

[11] G. P. Li, R. P. Hou, P. Z. Wang, and X. Z. Fan, "A test for pickling process of S31803 austenite-ferrite duplex phase stainless steel," *Special Steel*, vol. 29, pp. 67-68, 2008.

[12] L.-F. Li, Z.-H. Jiang, and Y. Riquier, "High-temperature oxidation of duplex stainless steels in air and mixed gas of air and CH_4," *Corrosion Science*, vol. 47, no. 1, pp. 57–68, 2005.

[13] S.-Y. Liu, C.-L. Lee, C.-H. Kao, and T.-P. Perng, "High-temperature oxidation behavior of two-phase iron-manganese-aluminum alloys," *Corrosion*, vol. 56, no. 4, pp. 339–349, 2000.

[14] V. P. Zhdanov and P. R. Norton, "Growth of oxide films on metal surfaces: transition from parabolic to linear kinetics," *Applied Surface Science*, vol. 99, no. 3, pp. 205–211, 1996.

[15] L.-F. Li, M. Daerden, P. Caenen, and J.-P. Celis, "Electrochemical behavior of hot-rolled 304 stainless steel during chemical pickling in HCl-based electrolytes," *Journal of The Electrochemical Society*, vol. 153, no. 5, pp. B145–B150, 2006.

[16] L.-F. Li, P. Caenen, and J.-P. Celis, "Effect of hydrochloric acid on pickling of hot-rolled 304 stainless steel in iron chloride-based electrolytes," *Corrosion Science*, vol. 50, no. 3, pp. 804–810, 2008.

[17] N. Ipek, B. Holm, R. Pettersson, G. Runnsjö, and M. Karlsson, "Electrolytic pickling of duplex stainless steel," *Materials and Corrosion*, vol. 56, no. 8, pp. 521–532, 2005.

[18] D. Mandrino and Č. Donik, "Chemical-state information obtained by AES and XPS from thin oxide layers on duplex stainless steel surfaces," *Vacuum*, vol. 86, no. 1, pp. 18–22, 2011.

[19] J. M. K. Hildén, J. V. A. Virtanen, and R. L. K. Ruoppa, "Mechanism of electrolytic pickling of stainless steels in a neutral sodium sulphate solution," *Materials and Corrosion*, vol. 51, no. 10, pp. 728–739, 2000.

[20] X. W. Yang, A. P. He, and B. Z. Yuan, *High-Temperature Thermodynamic Data Solution Manual*, Metallurgical Industry Press, Beijing, China, 1983.